2022

Radiometric age dating of the Scamander Formation and underlying units of the Mathinna Supergroup, Scamander area, eastern Tasmania

Authors: E. Knight, K. Orth and S. Meffre
Date: 10/06/2022
Email: info@mrt.tas.gov.au
Website: www.mrt.tas.gov.au

REPORT No: TR28

Geological Survey Technical Report 28

Tasmanian Government

Mineral Resources Tasmania
Department of State Growth

Geological Survey Technical Report 28:

Radiometric age dating of the Scamander Formation and underlying units of the Mathinna Supergroup, Scamander area, eastern Tasmania

by E. Knight, K. Orth, and S. Meffre

Cover: Eva Knight examining interbedded sandstone and mudstone turbidite deposits of possible equivalents of the Scamander Formation. Sandstone portions of the beds in the lower (left) and middle sections of the road cutting are up to 1 m thick. Some sandstones are amalgamated without intervening mudstone.

While every care has been taken in the preparation of this report, no warranty is given as to the correctness of the information and no liability is accepted for any statement or opinion or for any error or omission. No reader should act or fail to act on the basis of any material contained herein. Readers should consult professional advisers. As a result the Crown in Right of the State of Tasmania and its employees, contractors and agents expressly disclaim all and any liability (including all liability from or attributable to any negligent or wrongful act or omission) to any persons whatsoever in respect of anything done or omitted to be done by any such person in reliance whether in whole or in part upon any of the material in this report. Crown Copyright reserved.

Tasmanian Government

Mineral Resources Tasmania

Department of State Growth
www.mrt.tas.gov.au

Radiometric age dating of the Scamander Formation and underlying units of the Mathinna Supergroup, Scamander area, eastern Tasmania

by E. Knight, K. Orth and S. Meffre
School of Natural Sciences - University of Tasmania

CONTENTS

FIGURES

TABLES

1.0 Introduction

Radiometric age dating of detrital zircons in sedimentary rocks across the Lachlan Orogen has provided insights into the history and provenance of the rocks of southeastern Australia. Many samples have been analysed in previous studies from NSW and Victoria (e.g. Squires et al., 2006) but there are few studies of the detrital zircons in sedimentary rocks of the Mathinna Supergroup, comprising most of the southern part of the Lachlan Orogen in NE Tasmania.

A collaborative University of Tasmania–MRT research project generated new U-Pb radiometric ages of detrital zircon within the upper Mathinna Supergroup near Scamander on the east coast of Tasmania. A total of nine samples were collected and three were chosen for dating analyses. The new data add significant information on the provenance of the Panama Group and are the first from the youngest rocks in the Mathinna Supergroup in Tasmania.

The new data allow comparison of sources for the upper Mathinna Supergroup with other dated samples from lower in the Mathinna Supergroup, elsewhere in Tasmania and further afield to help understand the tectonic development of eastern Tasmania.

Previous work, the background geology, and previous constraints on the age of the Mathinna Supergroup are summarised in section 2. The sampling rationale and details of the three selected samples are described in section 3. The age data is presented in section 4. Comparisons of the new data with other datasets is discussed in section 5 and the implications of the new information summarised in the conclusion, section 6. Four appendices describe of all the samples (Appendix 1), outline the sample preparation and dating methods (Appendix 2), provide images of mounts and zircons (Appendix 3) and present all the zircon data (Appendix 4).

2.0 Background geology and ages of the Mathinna Supergroup

2.1 Geology and stratigraphy of the Mathinna Supergroup

The Mathinna Supergroup makes up a large portion of eastern Tasmania (Figure 1), comprising a 7 km thick succession of turbiditic units of consolidated sandstone and mudstone (Powell et al., 1993; Reed 2001).

Reed (2001), Bierlein et al. (2005) and Seymour et al. (2011) provide evidence to divide the Mathinna Supergroup into two separate units (Figure 2). The older Tippogoree Group in the west was affected by a Silurian deformation and separated from the overlying Panama Group by an unconformity. The Tippogoree Group includes the Stony Head Sandstone and the predominantly fine-grained Turquoise Bluff Slate. Seymour et al. (2011) recognised four units within the Panama Group. From base to top these are the Yarrow Creek Mudstone, the Retreat Formation, the Lone Star Siltstone and the Sideling Sandstone. The Scamander Formation is considered a lateral equivalent of the upper portions of the Sideling Sandstone (Calver et al., 2014). The Scamander Formation is a turbidite package with thick sandstone units. It is faulted in the west against fine-grained units of the Sideling Sandstone and extends eastwards to the coast at Scamander (Worthing and Woolward, 2010a) (Figure 3). It is unconformably overlain in the south by the St Marys Porphyry (Turner et al., 1986; Worthing and Woolward, 2010a).

2.2 Age from fossils in the Mathinna Supergroup

Sparse fossils constrain the age of the Mathinna Supergroup. Middle Ordovician graptolites were identified from the Turquoise Bluff Slate in the Pipers River area (VandenBerg in Reed 2001). Higher in the succession, graptolites were reported from the Golden Ridge area in the Panama Group northwest of St Helens (Rickards et al., 1993). These graptolites were deposited during the Ludlow of the middle-late Silurian (427 – 423 Ma). The youngest fossils from near Scamander also include graptolites. These graptolites are identified as *Monograptus aequabilis cf. notoaequabilis* by Rickards and Banks (1979) indicating a Pragian (410 – 407 Ma) age. Recent reviews of this graptolite in other successions (Lenz, 2013; Chen et al., 2015) led to a renaming of this species to *Neomonograptus notoaequibalis*. It is recognised as part of the *yukonensis* Biozone, within the Pragian (410 – 407 Ma) to early Emsian (407 – 393 Ma) the youngest known zone of planktonic graptoloids before they became extinct in the middle Devonian (Koren and Rickards, 1979).

2.3 Radiometric dating of the Mathinna Supergroup

Only three units have undergone U-Pb zircon radiometric dating in the Mathinna Supergroup and only one is from the Panama Group. The most recent analysis is from the Turquoise Bluff Slate (Berry et al., 2019) within the Tippogoree Group. Black et al. (2004) reported on two samples in NE Tasmania from the Stony Head Sandstone and the other from the sandstone in probably the Panama Group near the Queen of the Earth Gully close to the Golden Ridge fossil site (Black et al., 2004).

Results from the Panama Group sample (Black et al. 2014) indicates a predominance of younger zircons sourced from late Proterozoic to Cambro-Ordovician magmatism (650 – 450 Ma, 1000 – 750 Ma, 1250 – 1100 Ma) with a few older crystals from earlier in the Proterozoic (1350 Ma, 1700 Ma, 1800 Ma, 1850 Ma, 2300 Ma) and the Archean (2700 Ma). In comparison,

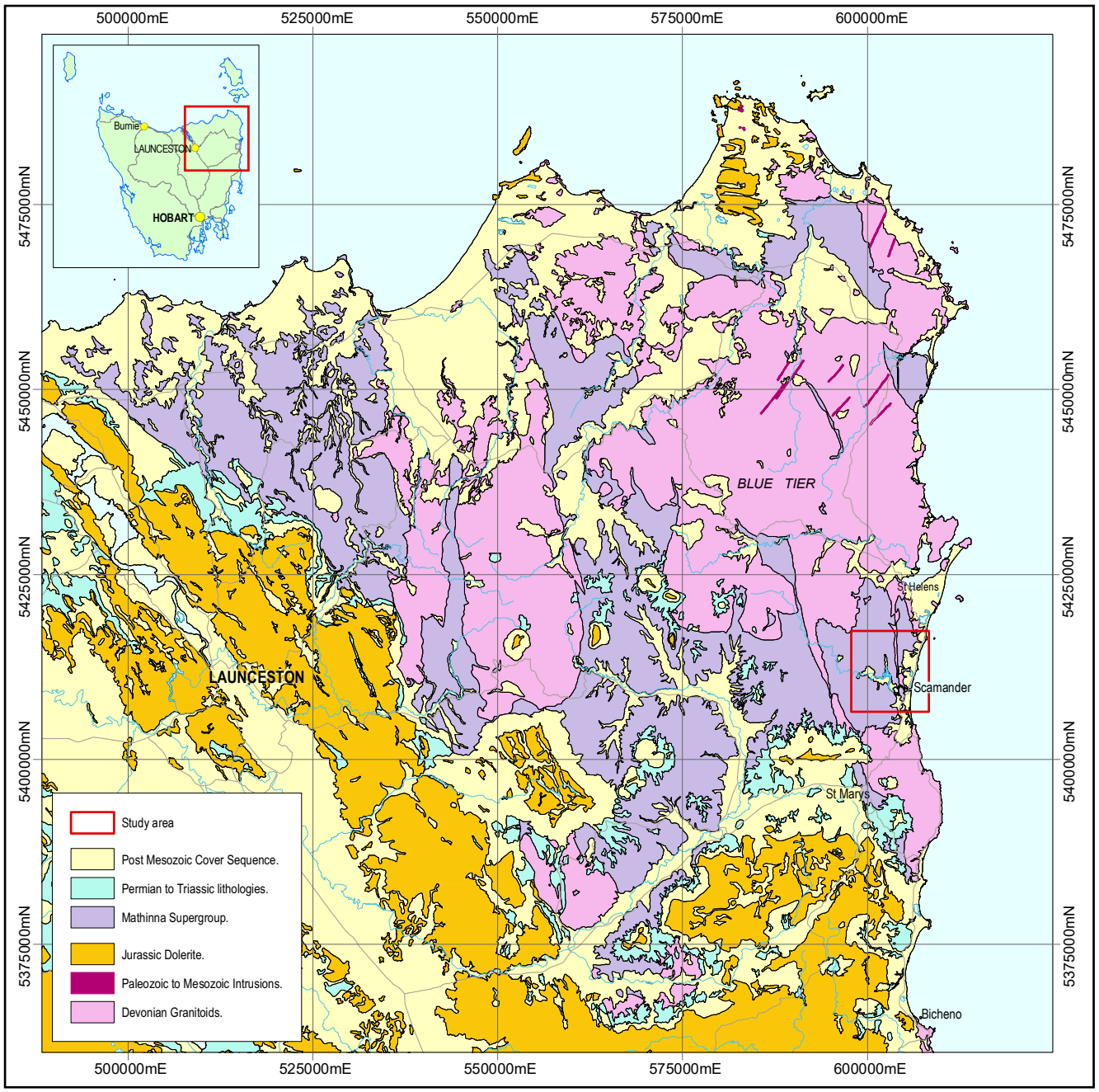

Figure 1. Geology of NE Tasmania (from 1:500 000 Map, Brown, et al., 2021). Purple = Mathinna Supergroup; Pink=intruding granitoids; Blue, green and orange =overlying Tasmania Basin; Yellow=younger sediment and basalt. Red box refers to sample area).

the oldest Tippogoree Group sample has a similar abundance of late Proterozoic and Cambrian zircons but with different ages for older crystals. Black et al. (2004) suggest that the sample is like sedimentary rocks elsewhere in the Lachlan Orogen but different to rocks in western Tasmania. Although zircons analysed by Berry et al. (2019) display a similar distribution to the samples of Black et al. (2004), confirming affinities at this time with the eastern Gondwana margin provenance (Squires et al., 2006), more 1800-1500 Ma zircons led them to interpret an input from zircons of western Tasmania in the Turquoise Bluff Slate.

3.0 Sampling

3.1 Samples

Nine sandstone samples were taken in the Scamander area (Table 1, Appendix 1). All come from coarse, sand-rich portions of turbidite deposits. Three were obtained from three thick sandstone units at different stratigraphic levels in the disused quarry next to the Scamander River where fossils including brachiopod and coral fragments were described by Rickards and Banks (1979). Two samples are from thick sandstone in the road cuttings of the Scamander Formation along the upper Scamander Road and two samples come from near the fossil location described by Rickards and Banks (1979) near Skyline Road northwest of Scamander. All these samples are considered to be in the Scamander Formation.

Two samples are from sandstone in turbidite packages that Worthing and Woolward (2010a) considered to be older than the Scamander Formation. One is from Bolpey Creek about 100 m west of the Semmens Road bridge and the other is from a road cutting on Semmens Road north of Bolpey Creek.

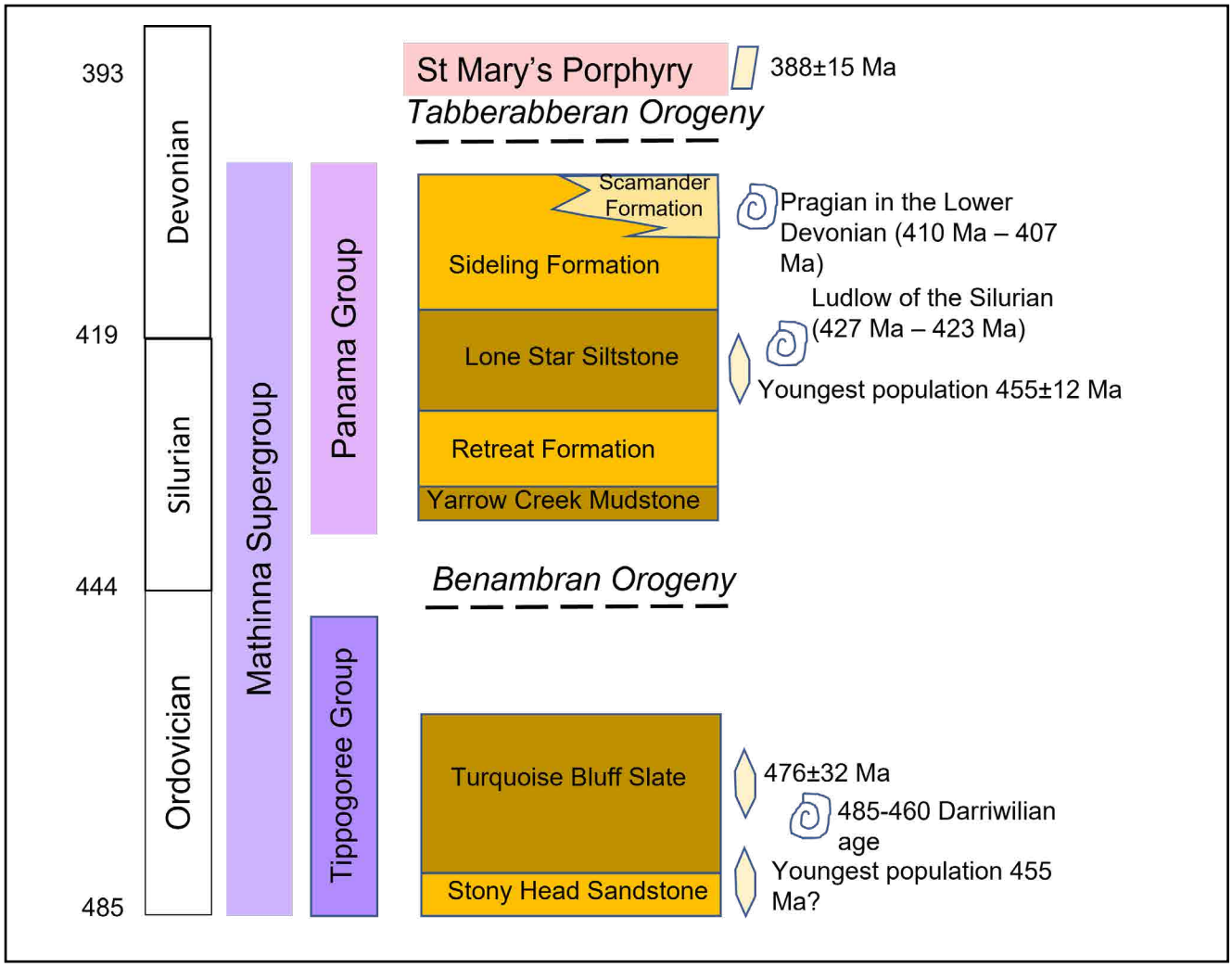

Figure 2. Simplified stratigraphic column, showing pre-existing fossil and zircon ages of the Ordovician to Devonian Mathinna Supergroup of Eastern Tasmania (Reed, 2001; Seymour et al., 2011; Berry et al., 2019).

Table 1. Sample locations and site descriptions.

Field No.	MRT No	General Location	Mathinna Supergroup Formation	Lithology	Zone	East	North	Comments
EK001	G409718	Scamander Quarry	Scamander Formation	Quartz rich medium grained sandstone	55G	605401	5409193	Carbonaceous spots - possible plant fossils, found in 6m of amalgamated sandstones.
EK002		Scamander Quarry	Scamander Formation	Silicified sandstone	55G	605385	5409174	Taken at base of approximately 1m-thick sandy unit; silica veins present.
EK003		Scamander Quarry	Scamander Formation	Medium to fine grained sandstone	55G	605362	5409185	From the base of 40cm-thick bed in a sequence of thick amalgamated sandstone beds; heavily vegetated.
EK004		Off Skyline Road		Medium to fine grained sandstone	55G	603462	5412063	Near Rickard and Banks (1979) graptolite location.
EK005	G409719	Upper Scamander Road	Scamander Formation	Medium to coarse sandstone	55G	602789	5409518	Laminations, flute casts and flame structures in turbidites with upwards fining cycles.
EK006		Upper Scamander Road	Scamander Formation	Medium to coarse sandstone	55G	602765	5409595	Taken from base of 1m-thick bed from second package of thick amalgamated sandstone; some feldspars present.
EK007		Bolpey's Creek		Fine grained sandstone	55G	599113	5408261	Interbedded dark grey shale and sandstone. From 20-30cm-thick beds surrounded by 15cm thick mudstone.
EK008	G409720	Semmen's Road Cut		Medium grained sandstone	55G	599176	5408844	356/50E, middle sequence of sandstones in road cutting.
EK009	G409721	Off Skyline Road		Medium to fine silicified sandstone	55G	603497	5412017	335/47W on track 193m off Skyline Road, at Rickard and Banks (1979) graptolite location; thickest (50 cm thick) sandstone bed

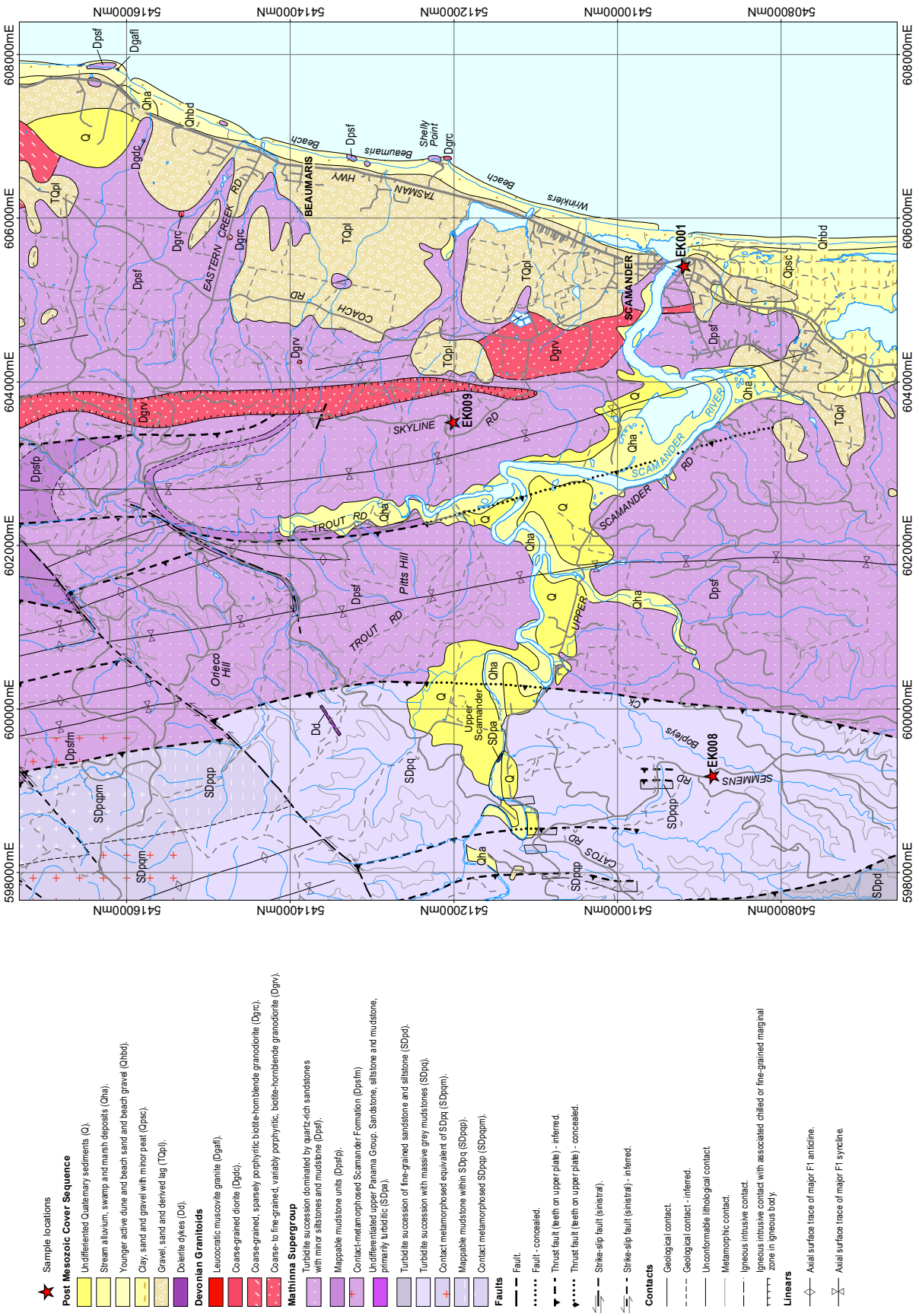

Figure 3. Geology of the Scamander area showing the main units and the sample locations (accurately) taken from Beaumaris, Brilliant, Falmouth and Dublin Town 1:25 000 geology maps. The unit in the west is part of the Sideling Formation and east of the fault in redder purple colour is the Scamander Formation. The red colours are the Scamander Tier Dyke and the browns and yellow are younger Cenozoic cover sediments (Worthing 2010a, b; Worthing and Woolward 2010b, c).

3.2 Samples for radiometric dating

Three samples, EK001, EK008 and EK009 were selected for their geological significance in representing the Scamander Formation (EK001, EK009) and the formation underlying it (EK008) (Figure 3). EK001 is a clean quartz-rich sandstone from the eastern end of the Scamander Quarry. EK009 was collected on a forestry track, off Skyline Road close to where Rickards and Banks (1979) collected their graptolites.

EK008 from the Semmens Road cutting north of Bolpey Creek was selected as one of the slightly older units in the area, faulted against the Scamander Formation.

3.3 Descriptions of dated samples

3.3.1 EK001 (G409718)

EK001(G409718) is a light grey coloured, coarse sandstone dominated by quartz clasts. Well to moderately sorted, with some large, rounded grains (<2 mm) and smaller clasts (<0.5 mm). Minor muscovite (< 2 mm) and weathered light brown clasts are often associated with light brown patches. Scattered throughout the rock are black carbonaceous fragments up to 20 mm long. Whitish cement is apparent in places as well as holes where some grains have been removed or weathered out.

In thin section, the rock contains portions that are well sorted and even-grained and other portions that display bimodality. Some of the larger grains (<2 mm) are composite sedimentary grains (Figure 4). Common quartz is most abundant along with sedimentary quartz displaying quartz overgrowths.

Some vein quartz is apparent as well as volcanic quartz grains. Lithic fragments are fine-grained, sedimentary clasts with some possible volcanic fragments and can be partially or wholly white-mica/clay-altered. Some of these clasts have been moulded between quartz grains along with a few larger sedimentary white mica grains. Biotite is within some common quartz grains. Irregular-shaped opaques are organic matter. Accessory minerals include well rounded, green and yellow tourmaline (Figure 4) and few scattered rounded and fragments of magmatic-shaped zircons crystals.

Interpretation

The quartz-dominated nature of the sandstone indicates that it is derived from mature sediment. The clasts reflect input from a predominantly sedimentary rock source with granite and vein quartz, some of which may be recycled and input from volcanism. The bimodality could be from the disaggregation of sedimentary rocks, or some sorting process, such as shoreline process prior to redeposition via turbidites into a deeper basin. The clay-rich fragments are fine-grained weathered material that were probably originally fine-grained sedimentary or volcanic lithic clasts and were subsequently altered by regional low-grade metamorphism (e.g. Patison et al., 2001). Carbonaceous fragments are plant fragments (Rickard and Banks 1979).

3.3.2 EK008 (G409720)

EK008 (G409720) is light yellow to brown, fine-medium grained sandstone with some patchy weathering. Quartz is the dominant component, but there are abundant brown weathered clasts and dark, possibly lithic fragments (20-30%). Grains are subangular and surrounded by a fine-grained yellow-brown matrix. A few white mica flakes are scattered throughout.

In thin section, angular to subangular and less abundant rounded clasts are within a light-brown altered matrix. Quartz clasts can display domanial and undulating extinction, but many appear to be common quartz. Some quartz have abundant vacuole trails indicative of vein quartz. Less abundant are uniform extinction quartz that may be volcanic quartz. Plagioclase feldspar is present but not abundant (Figure 5). The matrix appears to be compressed, poorly defined fragments of fine-grained sedimentary rocks and less common fine-grained volcanic clasts. Most are entirely composed of altering clay-white mica with very fine-grained iron oxides. A few of these have altered larger white mica flakes. Small accessory tourmaline and zircon (<0.05 mm), including some euhedral grains are scattered throughout.

The iron oxide appears to be altering what may have been iron-rich grains and associated with the formation of white micas from clays. Some iron oxide is also around clasts as a cement (Figure 5). In some parts of the sample, secondary carbonate is associate with the clay/white mica matrix.

Interpretation

The sandstone contains abundant angular to subangular quartz and lithic fragments and so is derived from submature sediment. Most quartz is derived ultimately from granite, quartz veins and volcanic sources. Lithic fragments are fine-grained, weathered sedimentary fragments which appear to be moulded during deformation and low-grade metamorphism around harder quartz clasts. These form a pseudomatrix. Secondary iron oxide, carbonate and clays formed during diagenesis and low-grade metamorphism.

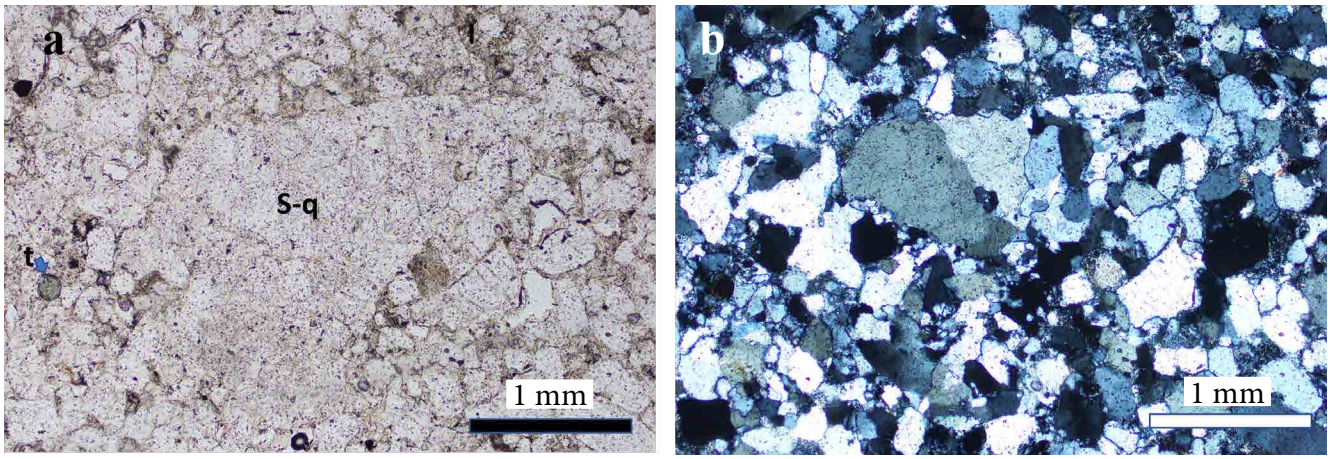

Figure 4. PPL (a) and XPL (b) of EK001 showing a large sedimentary quartz clast (S-q) surrounded by smaller quartz fragments and fine grained, sedimentary lithic fragments (l). Accessory tourmaline (t). Field of view is 4 mm across.

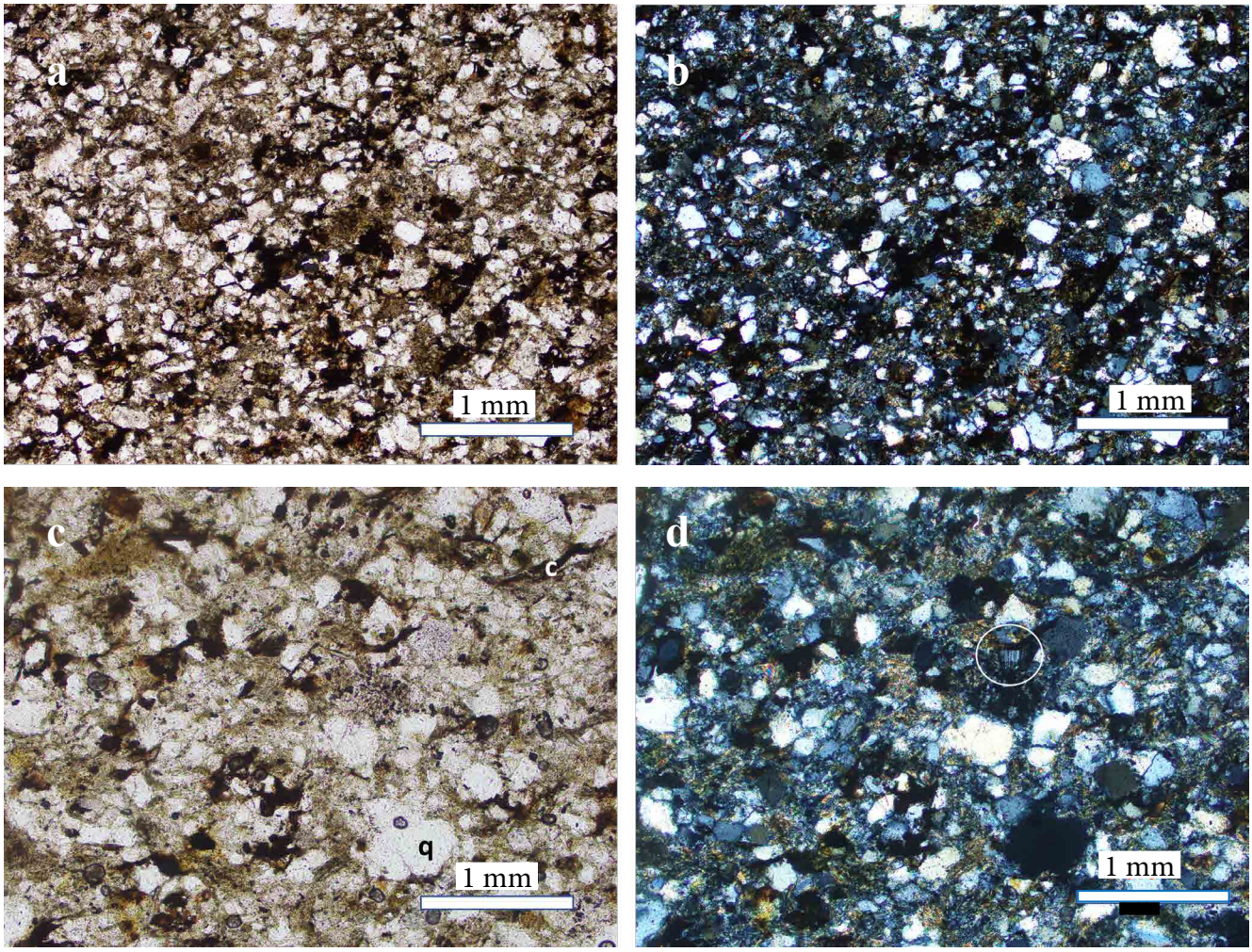

Figure 5. a) PPL and b) XPL images of EK008 showing abundant angular to subangular quartz clasts (clear in the PPL image) surrounded by lithic fragments that form an iron-oxide stained pseudomatrix Field of view is 4 mm across.
c) PPL and d) XPL images of dark brown grains and irregular patches of iron oxides. Most quartz grains are angular, common quartz (q) or vein quartz with some volcanic quartz. Rare feldspar is circled in the XPL image. The matrix is iron oxide-stained, fine-grained clay/micas replacing fine-grained sedimentary clasts and in places white mica clasts. In some places the iron oxide forms cement (c). Field of view is 2 mm.

3.3.3 EK009 (G409721)

EK009 is a well sorted, grey, medium grained sandstone. Quartz grains are dominant, but white altered areas comprise 20% of the rock. Some of these appear to be lath-like and are weathered light yellow to orange. Black clasts may be lithic or plant fragments and vary in shape. Several are elongate, but many are rounded. Most are less than 0.5 mm diameter, but some are up to 1 mm long.

In thin section, there appear to be different beds of fine and medium-grained sandstone. All are quartz dominated with the clasts ranging from subangular to rounded. Most of the quartz is common quartz. Some quartz grains display abundant vacuoles and may be vein quartz and some quartz is made up of many quartz subdomains that look like low-grade metamorphic clasts. These vary in subgrain dimensions and size. Some are fine-grained and others coarse grained (Figure 6). Many grains are elongate and some grains have elongate quartz subdomains. Clay/white mica rich lithic clasts are between the quartz grains. These can be partially moulded by surrounding grains and vary in shape. Some comprise all fine-grained white mica and can be lath-like in shape. The lithic fragments also include a few porphyritic felsic volcanic clasts.

Accessory zircons can form bands and although many are subhedral, all are rounded or fractured (Figure 6).

Interpretation

The grain shapes and composition in this medium to fine-grained sandstone indicate that the sediment redeposited to form the sandstone was relatively mature. Most abundant are deformed metamorphic fragments, some displaying elongate quartz subdomains. Some zircons form a heavy mineral band, suggesting some internal sorting process during deposition or cryptic bedding. Less abundant clay-rich lithics and possible detrital mica were compressed during burial compaction and were altered to fine-grained white micas during post-depositional, low-grade metamorphism.

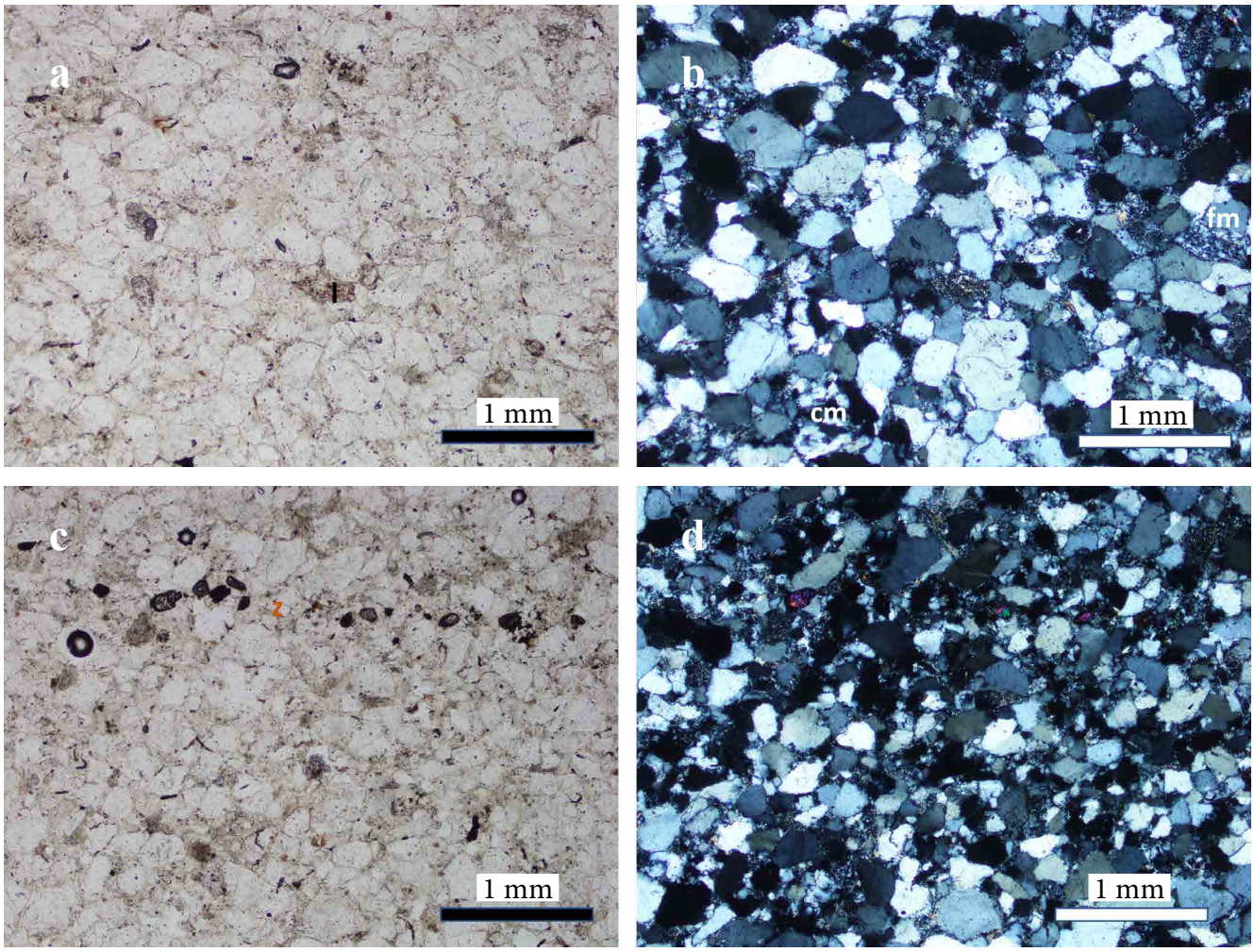

Figure 6. a) PPL and b) XPL images of EK009 showing abundant rounded to well-rounded mainly common quartz clasts, low grade coarse (cm) and fine-grained (fm) quartz-dominated metamorphic grains and clay-rich sedimentary to low grade metamorphic fragments (l). c) PPL and d) XPL images showing zircon-rich layer forming a heavy mineral band (z). Zircon crystals are all slightly rounded or fractured and have a high relief (left) and high birefringence (right). Field of view is 4 mm across in all images

4.0 Results of the U-Pb Zircon dating

U-Pb isotope analysis of about 70 zircons from each of the three samples EK001, EK008 and EK009 was undertaken at Earth Sciences, University of Tasmania using LA-ICPMS on polished mounts. To make these mounts the samples were crushed and milled and zircons were separated from the crushed samples. The zircons were mounted in two different ways; 30 large zircons were picked using a needle from the mineral separate and the remainder of the zircons were poured directly from the heavy mineral concentrates. Details of the methods used is in Appendix 2. All the mounts were examined prior to the analyses using SEM CL in the Central Science Laboratories at the University of Tasmania. Detailed images of the mounts are in Appendix 3 and all analyses are presented in Appendix 4.

4.1 Sample EK001

Many of the hand-picked zircons had clear magmatic shapes (Figure 7). The rest from the "poured" portion of the mount were more varied in shape and included more fragments of crystals. The poured portion of the mount also included many metamict zircons, that are black in CL (Figure 7). These metamict grains were not analysed.

Of the 70 zircons analysed for EK001 around 20 were rejected due to either discordance or due to the analyses showing evidence of Pb loss (e.g. high U zones within a single analysis containing young apparent Pb/U ages). A weighted average crystallisation age was calculated from the three youngest zircons from sample EK001 indicating a maximum deposition age of 397.2±8.8 Ma (2 sigma) (Figure 8).

The majority of the zircons in the sample formed during the Cambrian to Middle Devonian ranging from 510 – 480 Ma and 440 – 385 Ma. Some older zircons crystallised around 1100 Ma, with a few around 1650 Ma and the oldest at 2400 Ma (Figure 8). There were no Archean zircons in this sample.

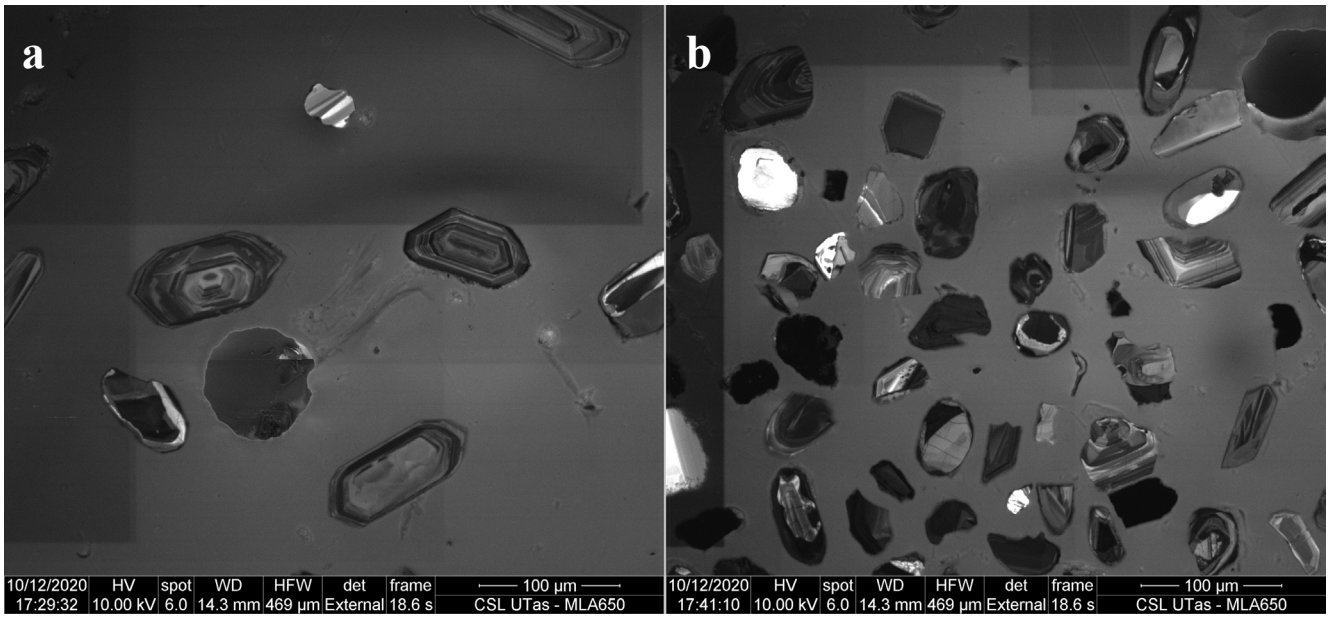

Figure 7. CL images of zircons in EK001 a) CL of euhedral zircons which were hand-picked. b) CL of the poured zircons which include zircons fragments, rounded crystals, some showing zonation and others that are dark are metamict.

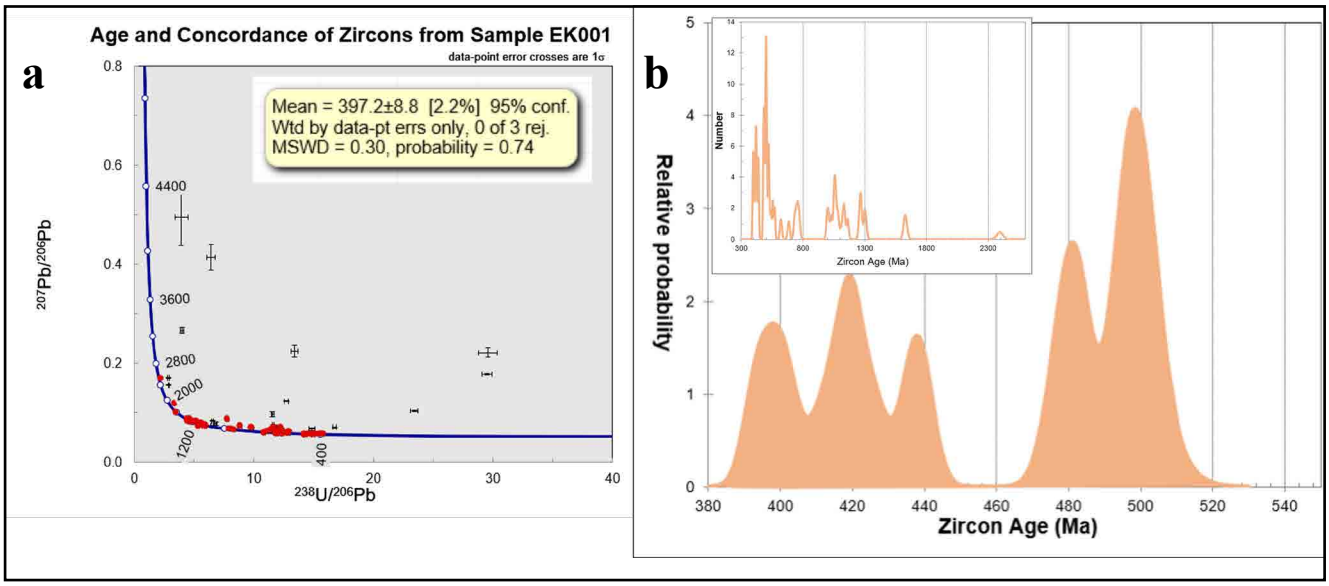

Figure 8. Radiometric age data for zircons from EK001. a) The concordance of each zircon in EK001 is measured by the Tera-Wasserberg plot showing the U-Pb zircon data. b) The youngest set of reliable zircons were used to construct a weighted average age. Sample EK001 contained the youngest zircons overall with an average age of 397.2±8.8. The inset shows the full spread of zircon ages in this sample.

4.2 Sample EK008

The zircons in this sample were similar to EK001 (Figure 9), except that more zircons appeared black in the CL images (Figure 9) indicating that more metamict zircons were present.

Twenty five of the 71 analyses for EK008 were not used as these were identified to contain Pb loss and/or strong discordance. The youngest four zircons in EK008 had indicated a maximum deposition age of 408.2 ± 6.6 Ma with a number of zircons spread up to 500 Ma (Figure 10). The sample also contained prominent zircon age peaks in the Proterozoic at 1100 – 900 Ma, 1700 – 1600 Ma, 2350 Ma and 2500 Ma with some Archean-aged zircons from 3100 Ma, 3200 Ma and 3600 Ma (Figure 10).

4.3 Sample EK009

Sample EK009 had the brightest zircons in the CL images but the shapes of the zircons were very similar to those described for EK001 (Figure 11).

Only five analyses were rejected outright from the 73 zircon crystals analysed from EK009. The weighted average age for the youngest six zircons indicate a maximum deposition age of 404.9 ± 5.4 Ma. Another population is between 500 – 480 Ma. (Figure 12). Proterozoic zircons include some that formed between 1200 – 600 Ma and aged from 1400 Ma, 1800 Ma, 2000 Ma and 2400 Ma, with a few that crystallised in the Archean at 2900 Ma (Figure 12).

Table 2 summarises the zircon data and indicates the number of analyses used to determine the maximum depositional age.

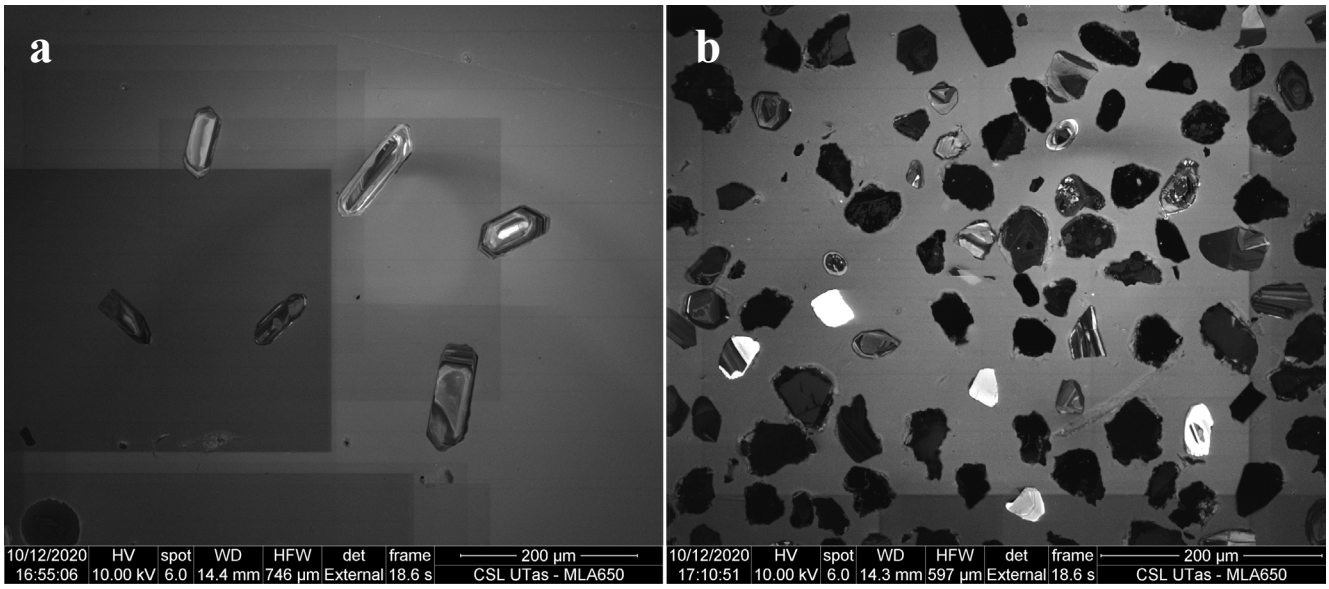

Figure 9. CL images of zircons in EK008. a) CL of euhedral zircons which were hand- picked. b) CL of the poured zircons which include zircons fragments, rounded crystals, some showing zonation and others that are dark and metamict.

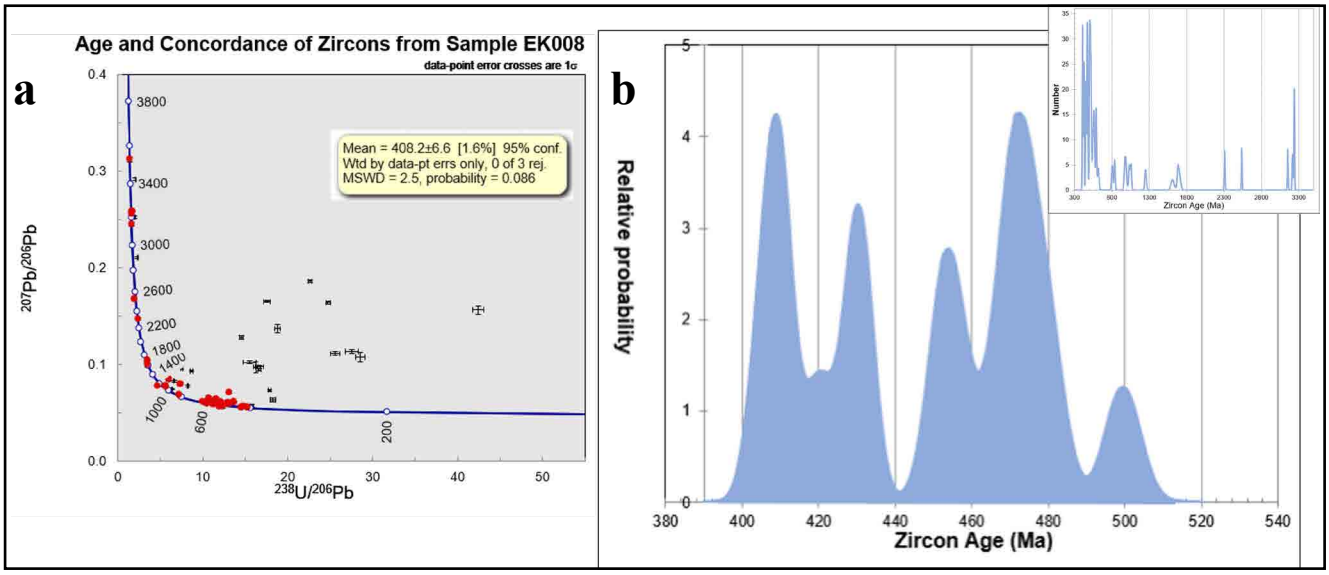

Figure 10. Radiometric ages and concordance of EK008 zircons. a) The concordance graph shows the high proportion of older zircons and a few younger than 500 Ma. b) Spread of ages shows the average age of the youngest zircons and the inset indicates that Archean zircons were incorporated into this rock.

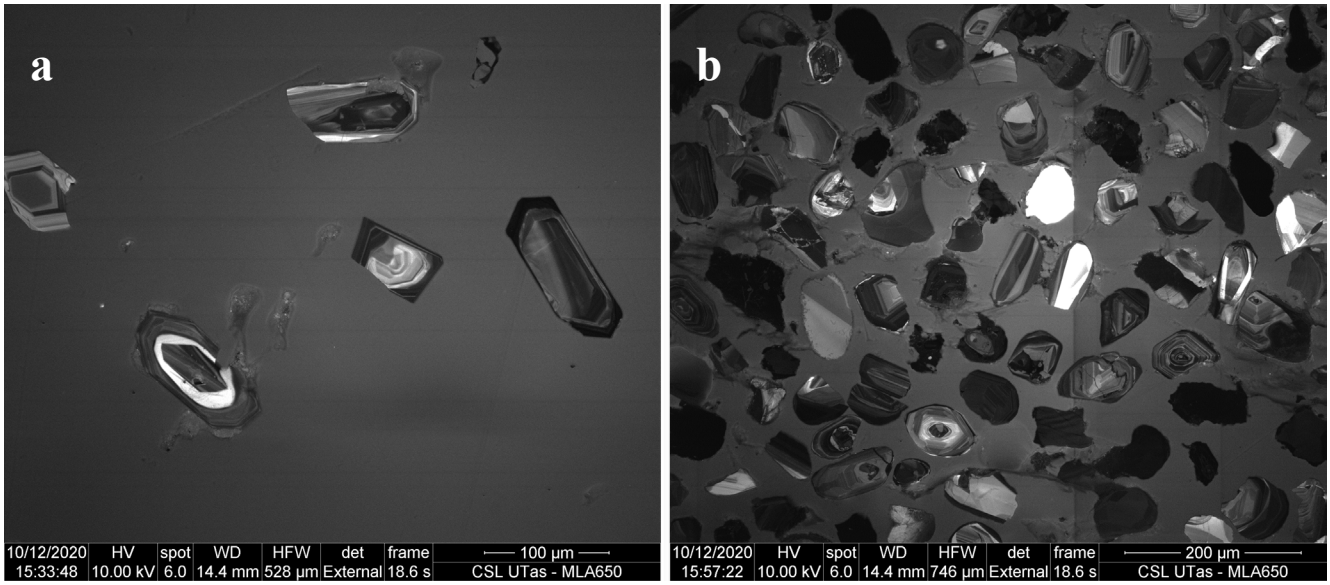

Figure 11. CL images of zircons in EK009. a) CL of euhedral zircons which were hand- picked. b) CL of the poured zircons which include zircons fragments, rounded crystals, some showing zonation and others that are dark and metamict.

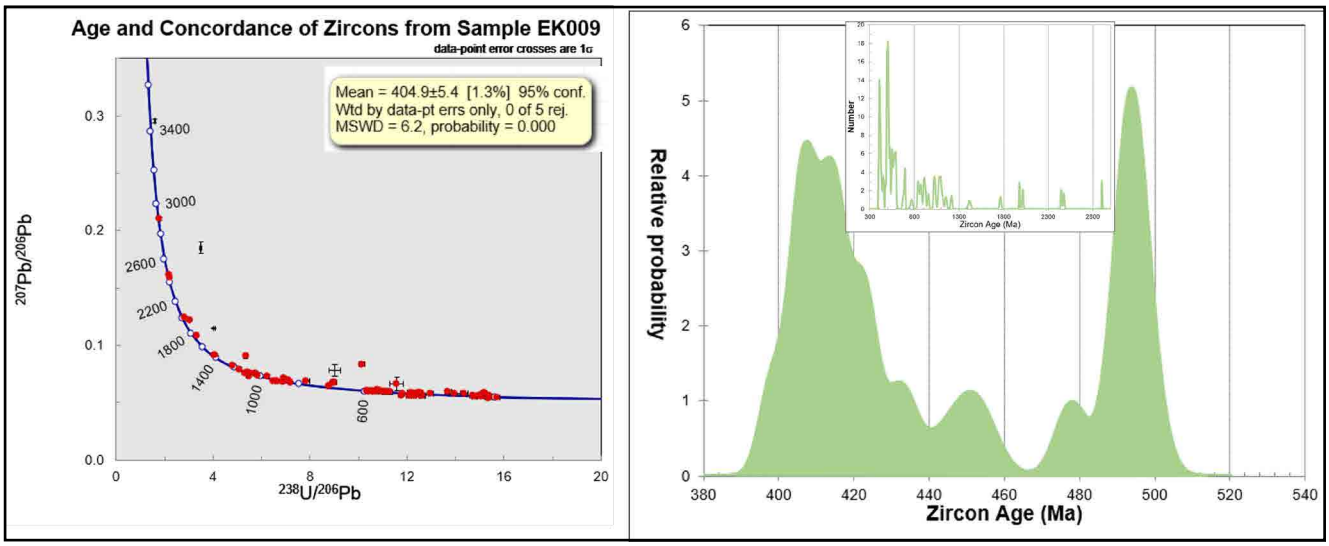

Figure 12. Radiometric ages and concordance of EK009 zircons. a) The concordance graph shows the high proportion of older zircons, with most younger than 600 Ma. b) Spread of ages shows the average age of the youngest zircons and the inset indicates that older Archean zircons were recycled into this rock.

Table 2. Summary of the zircon analyses.

MRT Sample No.	Field Sample No.	Youngest zircon Age (Ma)	Total Number of zircons	Number rejected	Number used in max dep age	Weighted mean max dep age (Ma)
G409718	EK001	393±4	71	19	3	397.2±8.8
G409720	EK008	405±4	72	26	4	408.2±6.6
G409721	EK009	398±3	74	4	6	404.9±5.4

5.0 Implications of the Age Dating

5.1 Comparison of zircon age data with fossil age information

Graptolite fossils Monograptus aequalibis notoaequabilis (now Neomonograptus notoaequibalis) (Rickard and Banks, 1979) indicate a Pragian (410 – 407 Ma) to Emsian (407 – 393 Ma) age for the Scamander Formation near EK009. The U-Pb dating age of the youngest zircons in all three samples overlap with this fossil age. The young age of the zircons indicates that the graptolites were contemporaneous with zircon formation and also suggest a short residence time for these young zircons in the sedimentary cycle.

5.2 Comparison to one another

Error bars for the weighted average of the youngest zircons in all three samples overlap and indicate that all the youngest zircons are lower to middle Devonian (Figure 13) indicating that deposition of the sedimentary rocks was either synchronous or post-dated this time frame. The sample collected from the youngest sample (EK001), from the uppermost part of the Scamander Formation also has the youngest maximum deposition age. Interestingly, this sample does not contain any Archean zircons. EK009 from lower in the Scamander Formation, has a maximum deposition age of 404.9 ± 5.4 Ma. The sample from lower in the stratigraphy EK008, has the oldest maximum deposition age at 408.2 ± 6.6 Ma and the most zircons older than 2000 Ma and the oldest zircons analysed.

Aside from the young Lower Devonian zircons, all three samples contain zircons formed in the Cambrian-Ordovician and common, but less abundant are Neoproterozoic zircons around 1100 – 900 Ma.

A few zircons are even older, formed around 1650 Ma and 1800 Ma and as old as 2400 Ma. Only the older two samples (EK008 and EK009) contain Archean zircons.

5.3 Comparison with other samples from the Mathinna Supergroup

The overall distribution pattern of a dominant early Paleozoic zircon population with some Neoproterozoic and minor other Proterozoic zircons in the three samples analysed is comparable with the distribution pattern of zircons in the Silurian Panama Group (Black et al., 2004), the older Tippogoree Group from the Stony Head Sandstone (Black et al., 2004) (Figure 14) and the Turquoise Bluff Sandstone (Berry et al., 2019). Black et al., (2004) suggested that although there were abundant Cambrian zircons in the older portions of the Mathinna Supergroup, these belonged to different populations, none of which were related to the 500 – 505 Ma Mt Read Volcanics in western Tasmania.

EK008 contains the oldest zircon (3600 Ma) analysed from the Mathinna Supergroup.

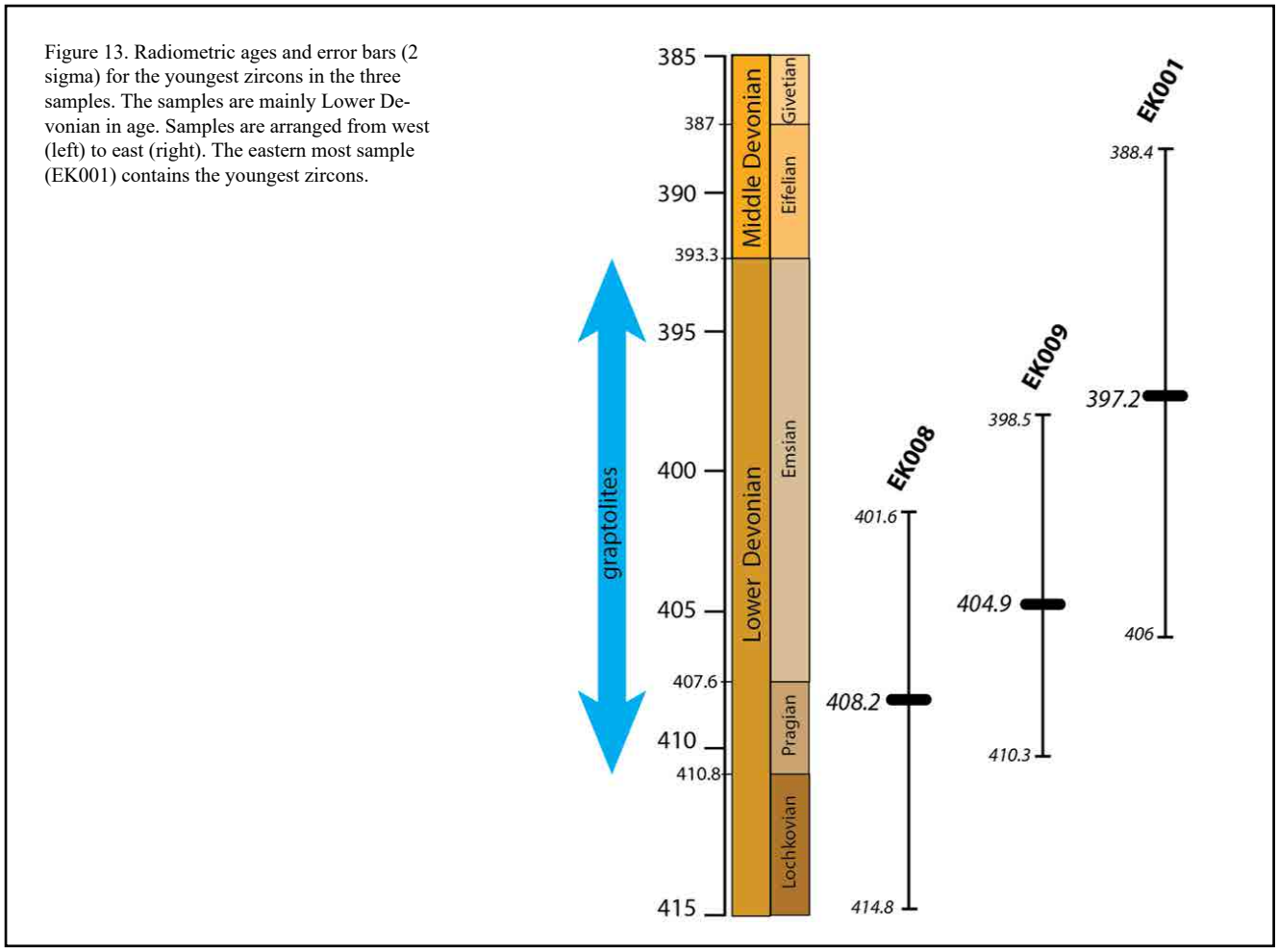

Figure 13. Radiometric ages and error bars (2 sigma) for the youngest zircons in the three samples. The samples are mainly Lower Devonian in age. Samples are arranged from west (left) to east (right). The eastern most sample (EK001) contains the youngest zircons.

5.4 Comparison with magmatic units in Eastern Tasmania

The youngest zircons in the uppermost sample EK001 from the Scamander Formation (397.2 ± 8.8 Ma) crystallised just before the overlying units of the St Marys Porphyry, which have a Rb-Sr age of 388 Ma (Turner et al., 1986). The young zircons in these sedimentary rocks overlap in age with the oldest granite plutons in the area, which have ages ranging from around 400 Ma to 390 Ma. These older intrusions include the Gardens, George River and Long Point granites in the Blue Tier Batholith (Black et al., 2005; Black et al., 2010; McClenaghan 2014; Hong et al., 2017) and granodiorite at Bluestone Bay farther south (Jones, 2017). Many other granites in the area are younger than 388 Ma (e.g. the Poimena Granite, much of the Scottsdale Batholith, Coles Bay Granite, parts of the Ben Lomond Granite and granite at Bicheno) (Black et al 2010; McClenaghan, 2014; Hong et al., 2017).

Progressive, or at least two-stages of, orogenesis and granite intrusion are apparent in the Tabberabberan Orogeny in Tasmania. This is indicated by the angular unconformity between the volcanic/magmatic St Marys Porphyry and the deformed underlying Mathinna Supergroup (Turner et al., 1986; Worthing and Woolward, 2010a). Some volcanism may have been associated with the early intrusions or a nearby convergent arc, which may have contributed to the sediment incorporated into the Scamander Formation.

Although the zircons' ages indicate provenance from early magmatism and some volcanic quartz and clasts are seen in EK001, most of the sediment was derived from more mature material than would be expected from a volcanic margin arc. If there was an arc, some of the arc-derived sediment was diluted by abundant continent-derived sediment or some processes reduced the preservation of less robust volcanic arc components.

5.5 Comparison to zircon provenance of the Lachlan Orogen in mainland Australia

The pattern of the zircon age of formation in all three sedimentary samples from the upper Panama Group are skewed to some late Neoproterozoic and abundant early Phanerozoic zircons. Although older zircons stretch back to the Mesoarchean, the Archean and early to middle Proterozoic zircons are less abundant. The pattern is similar to the distribution pattern of zircon ages in other sedimentary rocks across the Lachlan Orogen and indicate a similar provenance known as the 'Pacific Gondwana' signature derived from recycling Cambrian Delamerian rocks and Ordovician and younger Lachlan Orogen metasedimentary rocks (Ireland et al., 1998; Squires et al., 2006; Veevers et al., 2006; Haines et al., 2009; Shanaan et al., 2017; Asmussen, 2019).

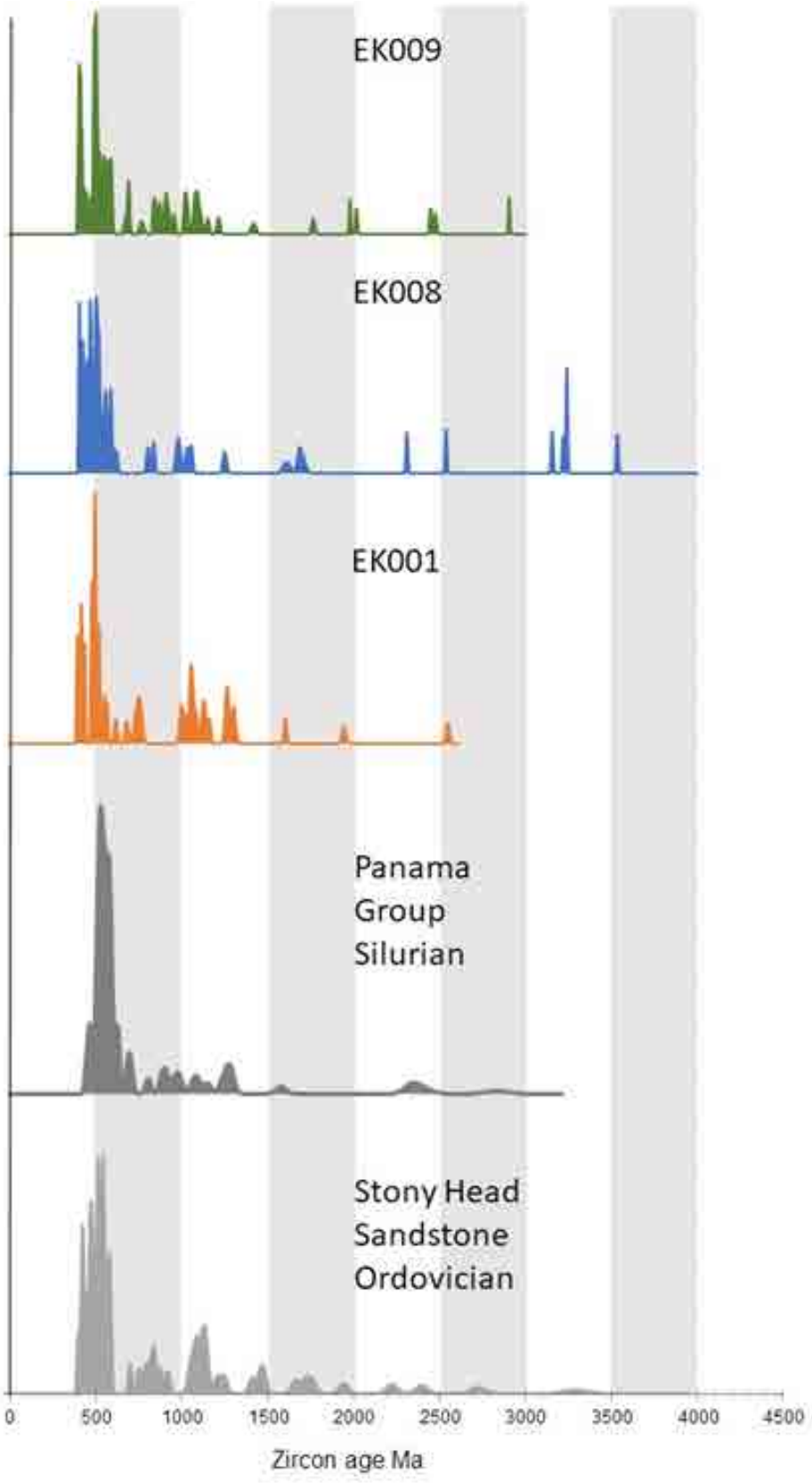

Figure 14. Data on zircon age populations for the Silurian Panama Group (dark grey), Stony Head Formation (light grey) both taken from Black et al. (2004), compared to EK001, EK008 and EK009. Although the overall patterns are similar, EK008 contained the oldest zircons reported from the Mathinna Supergroup.

6.0 Conclusions

All the samples for detrital U-Pb zircon age dating were collected from units deposited by turbidity currents during the Lower-Middle Devonian as constrained by Pragian graptolite fossils. Two were from the Scamander Formation and one from the unit possibly beneath it. The new data triple the published information on sedimentary zircons in the Panama Group and provide a lower limit on sedimentation of the youngest units in the Mathinna Supergroup. The crystallisation ages of the zircons indicate that the crystals accumulated in the sediment after the Lower to Middle Devonian. Although the error bars of all three samples overlap, the weighted mean average crystallisation age of the three samples is consistent with EK008 being from the lowest portion of the stratigraphy at 408.2 ± 6.6 Ma, EK009 from near the fossil location and within the Scamander Formation at 404.9 ± 5.4 Ma and the uppermost sample from the Scamander Quarry EK001, in the uppermost portion of the Scamander Formation at 397.2±8.8 Ma.

The young age of the youngest zircons is very close to the age of the fossils and indicates magmatism and deposition were almost contemporaneous. The close ages suggest that a source of magmatic zircons that were readily eroded was nearby. These maybe associated with local early magmatism, preserved in the area, or from a nearby volcanic arc.

Older zircons are similar in population distribution to older samples from the Panama Group and indicate an overall similar provenance. EK008, the lowest stratigraphically of these samples contains some Archean zircons, a few as old as 3600 Ma. These along with some from EK009, in the Scamander Formation, are the only samples analysed yet to contain such old zircons. The pattern of abundant zircons of Neoproterozoic and early Phanerozoic formation ages indicates a similar source to large sedimentary fans of the Lachlan Orogen and other Gondwana margin sedimentary basins.

7.0 References

Asmussen, P. 2019. *Insights from the Devonian Adavale Basin on the Tectonic History of the Thompson Orogen*. Unpublished Masters of Science thesis, Queensland University of Technology, 249 p.

Berry, R. F., Goemann, K., Thompson, J., Meffre S. and Bottrill, R. 2019. Geochemistry and provenance of the Turquoise Bluff Slate, northeastern Tasmania: tectonic significance, *Australian Journal of Earth Sciences*, 66: 227- 246.

Bierlein, F. P., Foster, D. A., Gray, D. R. and Davidson, G.J. 2005. Timing of orogenic gold mineralisation in northeastern Tasmania: implications for the tectonic and metallogenic evolution of Paleozoic SE Australia. *Mineralium Deposita,* 39: 890-903.

Black, L. P., Calver, C. R., Seymour, D. B. and Reed, A. 2004. SHRIMP U–Pb detrital zircon ages from Proterozoic and Early Palaeozoic sandstones and their bearing on the early geological evolution of Tasmania, *Australian Journal of Earth Sciences*, 51: 885-900.

Black, L., McClenaghan, M., Korsch, R. J., Everard, J. L. and Foudoulis, C. 2005. Significance of Devonian–Carboniferous igneous activity in Tasmania as derived from U–Pb SHRIMP dating of zircon. *Australian Journal of Earth Sciences*, 52: 807-829.

Black, L. P., Everard, J. L., McClenaghan, M. P., Korsch, R. J., Calver, C. R., Fioretti, A. M., Brown A. V. and Foudoulis, C. 2010. Controls on Devonian–Carboniferous magmatism in Tasmania, based on inherited zircon age patterns, Sr, Nd and Pb isotopes, and major and trace element geochemistry, *Australian Journal of Earth Sciences*, 57: 933-968.

Brown, A. V., (compiler). 2021 *Geology of Tasmania*. Edition 2021.1 Geological Atlas 1:500 000 digital series. Mineral Resources Tasmania.

Calver, C. R., Baillie, P. W., Banks, M. R. and Seymour, D. B. 2014. Ordovician-Lower Devonian successions. In: Geological Evolution of Tasmania, edited by K.D. Corbett, P.G. Quilty and C.R. Calver, *Geological Society of Australia Special Publication*, 24, pp.241-271.

Chen, X., Ni, Y., Lenz, A. C., Zhang, L., Chen, Z. and Tang, L. 2015. Early Devonian graptolites from the Qinzhou–Yulin region, southeast Guangxi, China. *Canadian Journal of Earth Sciences*, 52: 1000-1013.

Haines, P. W., Turner, S. P., Foden, J. D. and Jago, J. B. 2009. Isotopic and geochemical characterisation of the Cambrian Kanmantoo Group, South Australia: implications for stratigraphy and provenance. *Australian Journal of Earth Sciences*. 56: 1095-1110.

Hong, W., Cooke, D. R., Huston, D. L., Maas, R., Meffre, S., Thompson, J., Zhang, L. and Fox, N. 2017, Geochronological, geochemical and Pb isotopic compositions of Tasmanian granites (southeast Australia): Controls on petrogenesis, geodynamic evolution and tin mineralisation, *Gondwana Research*, 46: 124-140.

Ireland, T. R., Flottmann, T., Fanning, C. M., Gibson, G. M. and Preiss, W. V. 1998. Development of the early Paleozoic Pacific margin of Gondwana from detrital-zircon ages across the Delamerian orogen. *Geology*, 26: 243-246.

Jones, C. 2018. *Magmatic and magmatic hydrothermal transition textures at Bluestone Bay*. Unpublished Honours thesis, Earth Sciences, University of Tasmania, 103p.

Koren, T. N. and Rickards, R. B. 1979. Extinction of graptolites, In: The Caledonides of the British Isles - reviewed, edited by A. L. Harris, C. H. Holland and B. E. Leake, *Geological Society of London Special Publication*, 8, pp. 457-466.

Lenz, A. C. 2013. Early Devonian graptolite biostratigraphy, Arctic Islands, Canada. *Canadian Journal of Earth Sciences*, 50: 1097-1115.

McClenaghan, M. P. 2014. Devonian-Carboniferous granitic magmatism in Tasmania. In: Geological Evolution of Tasmania edited by K. D. Corbett, P. G. Quilty and C. R. Calver, *Geological Society of Australia Special Publication*, 24, pp. 296-318.

Patison, N. L., Berry, R. F., Davidson, G. J., Taylor, B. P., Bottrill, R. S., Manzi, B., Ryba, J. and Shepherd, R. E. 2001. Regional metamorphism of the Mathinna Group, northeast Tasmania. *Australian Journal of Earth Sciences*, 48: 281-292.

Powell, C. M. A., Baillie, P. W., Conaghan, P. J. and Turner, N. J. 1993. The turbiditic mid-Palaeozoic Mathinna Group, northeast Tasmania. *Australian Journal of Earth Sciences*, 40: 169-196.

Reed, A. R. 2001. Pre-Tabberabberan deformation in eastern Tasmania: A southern extension of the Benambran Orogeny, *Australian Journal of Earth Sciences*, 48: 785-796.

Rickards, R. B. and Banks, M. R. 1979. An Early Devonian monograptid from the Mathinna Beds, *Tasmania, Alcheringa*, 3: 307-311.

Rickards, R. B., Davidson, G. and Banks, M. R. 1993. Silurian (Ludlow) graptolites from Golden Ridge, north-east Tasmania. *Association of Australasian Palaeontologists Memoir,* 15: 125-135.

Seymour, D. B., Woolward, I. R., McClenaghan, M. P. and Bottrill, R.S. 2011. *Stratigraphic revision and remapping of the Mathinna Supergroup between the River Tamar and the Scottsdale Batholith, northeast Tasmania*, Mineral Resources Tasmania. 1:25 000 scale digital geological map series explanatory report, 4, 82p.

Squire, R., Campbell, I., Allen, C. and Wilson, C. 2006. Did the Transgondwanan Supermountain trigger the explosive radiation of animals on Earth? *Earth and Planetary Science Letters*, 250: 116-133.

Turner, N. J., Black, L. P., and Higgins, N. C. 1986. The St Marys Porphyrite—a Devonian ash-flow tuff and its feeder, *Australian Journal of Earth Sciences*, 33: 201-218.

Shaanan, U., Rosenbaum, G. and Sihombing, F. M. H. 2017. Continuation of the Ross–Delamerian Orogen: insights from eastern Australian detrital-zircon data, *Australian Journal of Earth Sciences*, 65: 1123-1131.

Veevers, J. J., Belousova, E. A., Saeed, A., Sircombe, K., Cooper, A. F. and Read, S. E. 2006. Pan-Gondwanaland detrital zircons from Australiua anaysed for Hf-isotiopes and trace elements reflect an ice-covered Antractic provenance of 700-500 Ma age TDM of 2.0-1.0 Ga and alkaline affinity, *Earth Science Reviews,* 76: 135-174.

Worthing, M. A. (compiler) 2010a. Digital Geological Atlas 1:25 000 Scale Series. Sheet 6041. *Beaumaris*. Mineral Resources Tasmania.

Worthing, M. A. (compiler) 2010b. Digital Geological Atlas 1:25 000 Scale Series. Sheet 6040. *Falmouth*. Mineral Resources Tasmania.

Worthing M.A. and Woolward I.R. 2010a. *Explanatory Report for the Dublin Town (5840), Brilliant (5841), Falmouth (6040) and Beaumaris (6041) geological map sheets, Mineral Resources Tasmania*. 1:25 000 scale digital geological map series explanatory report, 3, 75p.

Worthing, M. A. and Woolward, I. R. (compilers) 2010b. Digital Geological Atlas 1:25 000 Series. Sheet 5841. *Brilliant*. Mineral Resources Tasmania.

Worthing, M. A. and Woolward, I. R. (compilers) 2010c. Digital Geological Atlas 1:25 000 Series Sheet 5840. *Dublin Town*. Mineral Resources Tasmania.

APPENDICES

Located :
https://www.mrt.tas.gov.au/mrtdoc/dominfo/download/TR28/

Appendix 1 - Location and descriptions of samples EK001-EK009
-Download-

Appendix 2 - Zircon sample preparation, analyses and data reduction methods
-Download-

Appendix 3 - Cathodoluminescence images of zircon mounts EK001, EK008 and EK009
-Download-

Appendix 4 - Zircon analyses and calculated ages
-Download-

Tasmanian
Government

Mineral Resources Tasmania
PO Box 56 Rosny Park
Tasmania Australia 7018
Ph: +61 3 6165 4800

info@mrt.tas.gov.au www.mrt.tas.gov.au